Preprint Title	Batch preparation and characterization of ZnO/PLGA/PCL nanofiber membranes for antibacterial materials
Authors	Siqi Li, Jing Yin and Lan Xu
Publication Date	07 Juni 2021
Article Type	Full Research Paper
ORCID® iDs	Lan Xu - https://orcid.org/0000-0001-6391-6727

Batch preparation and characterization of ZnO/PLGA/PCL nanofiber membranes for antibacterial materials

Siqi Li, Jing Yin, Lan Xu*

College of Textile and Engineering, Soochow University, 199 Ren-ai Road, Suzhou 215123, China

*Corresponding authors: lanxu@suda.edu.cn (L. X.).

Abstract

As biomaterials with excellent biocompatibility, biodegradation and low toxicity, poly(ε-caprolactone) (PCL) and poly(lactic-co-glycolic acid) (PLGA) are widely applied as wound dressing and surgical suture in biomedical field. In this paper, an oblique section free surface eletrospinning (OSFSE) apparatus was utilized to prepare high-quality and high-output ZnO/PLGA/PCL nanofiber membranes (NFMs) for antibacterial materials. The effects of the weight ratio of PLGA and PCL on the viscosity and conductivity of electrospinning solutions as well as the yield, morphology and wettability of PLGA/PCL NFMs were researched, and the optimal weight ratio of 6:4 was determined. Then the effects of ZnO contents on the electrospinning solution properties as well as the yield, morphology, structure, wettability, mechanical property and antibacterial performance of ZnO/PLGA/PCL NFMs with the optimal ratio of PLGA and PCL were studied. The results indicated that the addition of ZnO could improve significantly the antibacterial effect of NFMs, and the NFMs with 3 wt% ZnO had excellent antibacterial activity against *E. coli* (95.3%) and *S. aureus* (95.7%).

Introduction

Poly(lactic-co-glycolic acid) (PLGA) has been widely used in various applications, such as wound dressing,[1] drug release,[2] bone tissue engineering[3] and artificial skin,[4] due to its excellent biocompatibility, biodegradation and low toxicity. However, the disadvantages of PLGA lie in poor mechanical property[5,6] and short degradation period[7] so that it can not satisfy the requirement of medical tissue materials. Poly(ε-caprolactone)/ (PCL) is a nontoxic, biodegradable and biocompatible polymer, which has been approved for biomedical applications, such as drug delivery,[8] medical apparatuses,[9] in vitro cell cultures[10] and biodegradable packing materials.[11] Due to its good mechanical properties and electrospinnability, PCL is often used as a functional component to improve the properties of eletrospun materials.[12,13] In natural environment, both PLGA and PCL can be completely degraded into environmentally friendly substances in a short time. The former can be degraded into lactic acid and glycolic acid,[14,15] while the latter can be degraded into carbon dioxide and water.[16-18] Therefore, the mechanical properties of PLGA can be improved by adding PCL. Moreover, since PLGA/PCL composites are susceptible to bacterial infection, it is necessary to find additives to enhance their antibacterial properties.[19]

Nano-ZnO is a kind of inorganic antibacterial materials, which has the advantages of wide source, economy, high safety and good durability.[20] Under the light condition, Nano-ZnO will be excited

by light to generate negatively charged free electrons as well as positively charged holes, and the generated holes has strong chemical activity and can convert the oxygen in the air into bactericidal reactive oxygen, resulting in good antibacterial effects of nano-ZnO.[21,22] However, due to its high specific surface area, small grain size and a lot of surface hydroxyl groups, nano-ZnO is prone to aggregation in the preparation of polymer-based nanomaterials, which may limit its effect.[23,24] Therefore, as a coupling agent, CA is often used to improve interaction between groups so as to reduce the aggregation of nanoparticles. And CA can modify the activity of nano-ZnO and inhibit the agglomeration of nanoparticles by forming ester bonds with hydroxyl groups on the surface of nano-ZnO.

Electrospinning (ES), a simple and effective technique for manufacturing polymer nanofibers, has been widely used in non-woven fabrics,[25,26] reinforced fibers,[27,28] drug controlled release,[29,30] tissue scaffold engineering,[30,31] and other fields.[32-34] However, the industrial application of conventional single-needle electrospinning is limited because of its low output, which is often only 0.01-0.1 g/h.[35] A lot of studies have focused on mass fabrication of high-quality nanofibers through ES technology, like multi-needle ES,[36,37] needless ES,[38,39] and free surface ES (FSE).[40] In our earlier studies,[41-46] some self-made FSE apparatuses were proposed to prepare NFMs in large quantities. In this paper, an oblique section free surface eletrospinning (OSFSE) apparatus, as shown in Fig.1, was used to fabricate high-output and high-quality ZnO/PLGA/PCL nanofibers membranes for antibacterial materials. The influences of various proportions of ZnO, PLGA and PCL on the properties of spinning solution were studied by investigating the solution viscosity and conductivity. And the morphology, structure, yield, mechanical property, wettability and antibacterial property of ZnO/PLGA/PCL NFMs with various proportions were illustrated to determine the optimum proportion.

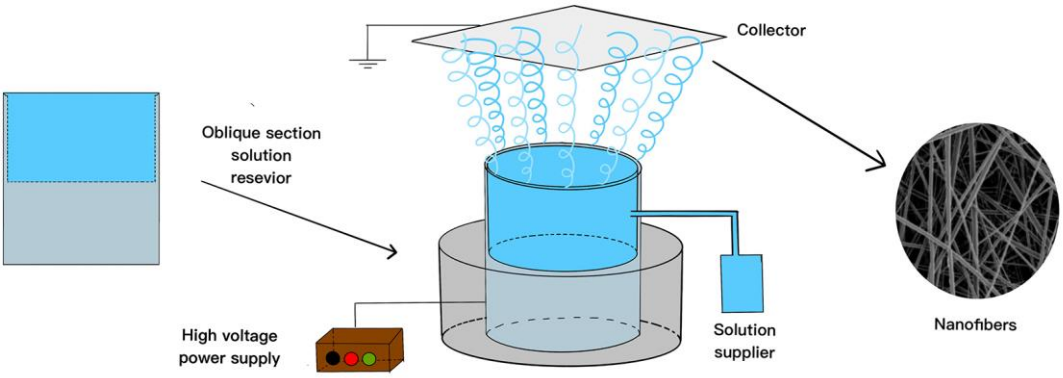

Figure 1 Schematic presentation of OSFSE

Materials and methods

Materials

Polycaprolactone (PCL, Mn=80 kDa) was supplied by Yuanye Biochemical Co., Ltd. (Shanghai, China). Poly(lactic-co-glycolic acid) (PLGA, molar ratio of lactide/glycolide equals 75/25, Mn= 100 kDa) was supplied by Daigang Biomaterial Co., Ltd (Jinan, China). Hexafluoroisopropanol (HFI) was purchased from Aladdin Bio-chem Technology Co., Ltd. Citric acid monohydrate (CA)

was supplied by Lingfeng Chemical Reagent Co., Ltd (Shanghai, China). Nano-ZnO was provided by Shenghehaoyuan Technology Co., Ltd (Beijing, China). Staphylococcus aureus (*S. aureus*) and escherichia coli (*E. coli*) for antibacterial experiments were provided by Soochow University. Nutrient agar and nutrient broth mediums were obtained from SCAS Ecoscience Technology Inc. Na_2HPO_4 and KH_2PO_4 were supplied by Sinopharma chemical reagent Co., Ltd. (Shanghai, China). All chemicals are analytical reagent grade and can be applied without purification.

Preparation of spinning solution

A certain amount of PLGA and PCL were dissolved in hexafluoroisopropanol (HFI) to prepare the mixed spinning solutions with the total solute concentration of 11wt%.[47,48] And the weight ratios of PLGA and PCL were 7:3, 6:4, 5:5, 4:6 and 3:7, respectively. The electrospinning solutions with various PLGA/PCL weight ratios were fabricated by mixing the solutions with a magnetic stirrer (HJ-6A, Yuhua Instrument Co., Ltd., Gongyi, China) for 12h. Then, the different contents of ZnO and CA were added into PLGA/PCL solution with the optimal PLGA/PCL weight ratio. The weight ratio of ZnO and CA remained 10:3,[49] and the concentration of ZnO relative to the total solute was 3 wt%, 5wt% and 7wt%, respectively.

OSFSE process and batch preparation of NFMs

As illustrated in Figure 1, the OSFSE apparatus mainly consists of a solution reservoir, a grounded collector and a high-voltage generator (0-150 kV, TRC2020, Dalian Teslaman Technology Co., Ltd). The volume of the copper solution reservoir is composed of a cylinder and a circular truncated cone, which makes the top edge of the solution reservoir an oblique section for better spinning. According our previous works,[41-46] the OSFSE parameters were set as follows: the applied voltages ranged from 40 to 56 kV and the working distance of spinning was 18 cm. The spinning processes were implemented at a relative humidity of 60% and 20℃.

The OSFSE processes were recorded by a high speed camera (VRI-Phantom-VEO-L, Ametek, California, USA), to observe the spinning effects of multiple jets under different voltages, as indicated in Figure 2. It was found that after applying the electric field force, the surface tension of the solution was overcome, leading to the generation of many jets on the surface of the solution. Then, the jets were stretched, elongated and formed into nanofibers on the collector. Furthermore, as the applied voltage increased, the electric field force enhanced gradually, which made more jets stretch from the spinning solution surface to form nanofibers. That meant the higher the applied voltage was, the more charged jets were produced, and the more nanofibers were obtained. However, excessive voltage (over 56 kV) would result in the electric field instability and the poor safety. Therefore, the voltage of 56kV was selected as the applied voltage in further studies.

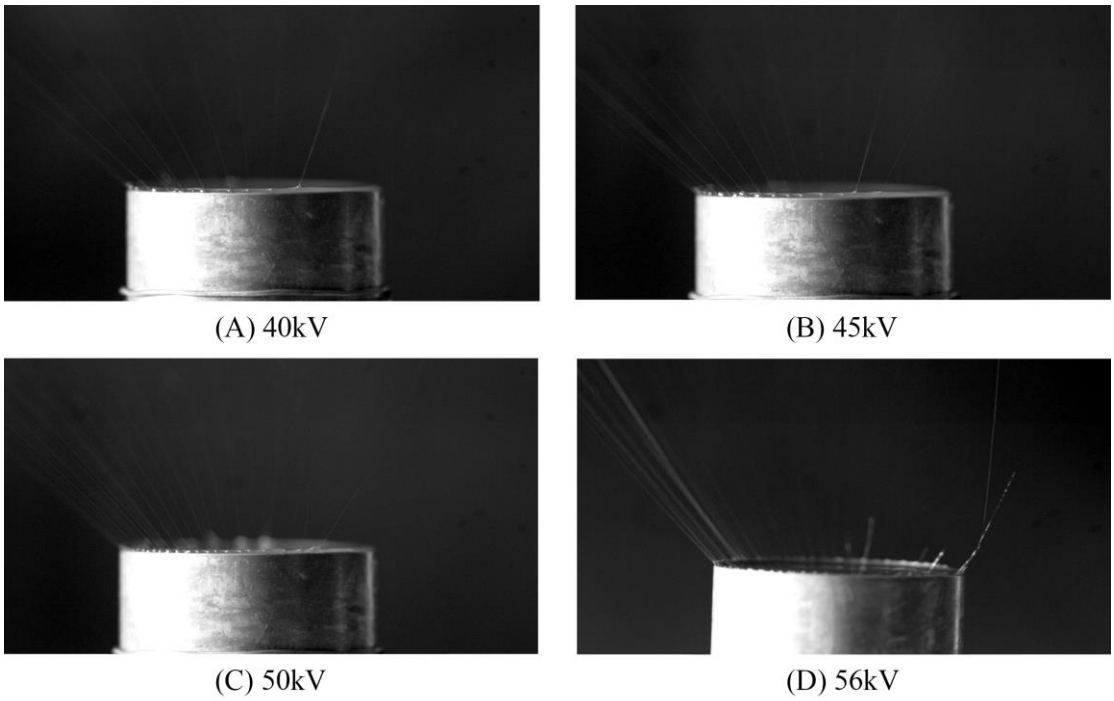

Figure 2 Images of OSFSE processes under different voltages.

Measurements and characterizations

Property of spinning solution

The solution viscosity and conductivity were determined by a viscometer (SNB-1, FangRui Instrument Co., Ltd., Shanghai, China) and a conductivity meter (DDS-307A, Shanghai IE Scientific Instrument Co., Ltd., Shanghai, China), respectively. The test was repeated five times at room temperature to obtain the average value.

Yield of NFMs

After spinning for 30 min under a stable condition, the NFMs prepared by OSFES apparatus was weighed using a precise electronic balance. And the test was repeated five times for obtaining the average value.

Surface morphology and element compositions of NFMs

The surface morphology of NFMs were observed by a scanning electronic microscopy (SEM, Hitachi S-4800, Japan), and the element compositions of the sample region was characterized through the energy dispersion spectroscopy (EDS, Hitachi S-4800, Japan). All samples were dried at 20℃, and then sputter-coated with gold for 90s to improve electrical conductivity of the NFMs. 10 SEM pictures of each sample and 100 nanofibers in each SEM picture were randomly selected and further analyzed by ImageJ software (National Institute of Mental Health, Nethesda, Maryland, USA) to investigate the diameter distribution of nanofibers.

ATR-FTIR of NFMs

To investigate the chemical characterization of PLGA/PCL/ZnO NFMs, the ATR-FTIR spectra of NFMs was measured by a Attenuated Total Reflection Fourier transform infrared (ATR-FTIR) spectroscopy (Nicolet5700, Thermo Nicolet Company, Wattham, MA, USA). The test parameters were an average of 32 scans, a spectral resolution of 4 cm^{-1} and a wavenumber range between 400 and 4000 cm^{-1} .

XRD of NFMs

The crystalline structure of NFMs were measured by a X-ray diffractometer (XRD, Philips X'Pert-Pro MPD, PANalytical, Holland). All samples were smoothed and placed on the sample plate. The test parameters were a voltage of 40 kV, a current of 40 mA, a radiation source of Cu target, a scan angle range of 5-80° and a scan speed of 2°/min.

Mechanical property of NFMs

The mechanical properties of NFMs were investigated by a universal electromechanical test machine Instro-3365 (Intro, Norwood, MA, USA). All samples were 40mm × 20mm NFMs and were placed at relative humidity of 60% and 20℃ for 24h to stabilize the structure of NFMs. The measure parameters were a pre-tension of 0.2 cN, a clamping length of 20 mm and a tensile rate of 100mm/min. The test was repeated five times for accuracy.

Wettability of NFMs

The water contact angle (WCA) measurement was carried out using a Kruss K100 device (Kruss Company, Hamburg, Germany) to indicate the wettability of NFMs. The samples were cut into 10mm×10mm square membranes and placed in a vacuum dryer overnight. The four corners of the sample were flattened by a glass slide to remove the impact of its surface on the test data. The volume of droplet used was 6μL. To make sure the accuracy, WCA measurement of each sample should be performed at five different positions on the same sample.

Antibacterial property of NFMs

The antibacterial activities of NFMs against *S. aureus* and *E. coli* were characterized. Phosphate buffered saline (PBS) was prepared by adding 2.84g Na_2HPO_4 and 1.36g KH_2PO_4 into 1 l deionized water. To alleviate the influence of irrelevant parameters on antibacterial tests, 150 mg test samples were disinfected by ultraviolet light for 1 h. Single colony was cultured for 18-24h in nutrient broth medium to obtain bacterial solution. 1 ml of bacterial solution and 9 ml PBS solution were mixed to prepare the diluted bacterial solution with the concentration of $3–5\times10^5$ colony forming units (CFU/ml).

150 mg test sample was put into the further diluted bacterial solution in a conical flask, which was composed of 1ml diluted bacterial solution and 14 ml PBS. And the flask was completely swayed in an incubator shaker (IS-RDV1, Crystal Technology & Industries, Inc., USA) for 18 h at 25℃

Afterwards, 1 ml of the prepared sample solution mixed with 20ml agar was poured onto a nutrient agar plate, which was put into thermostatic oscillator for incubation for 24 h at 37℃. Finally, the contamination condition was observed and the bacterial colony count was obtained. Furthermore, the antibacterial rate is calculated as follows:[42]

$$\text{Antibacterial rate}=(N_c-N_s)/N_c\times 100\% \quad (1)$$

where N_C is the bacterial colony count of standard cotton cloth after contacting with bacteria for 24 h, N_S is the bacterial colony count of ZnO/PLGA/PCL NFMs after contacting with bacteria for 24 h.

Results and discussion

Influences of the weight ratio of PLGA and PCL

PLGA/PCL NFMs with different PLGA/PCL weight ratios were prepared by OSFSE apparatus at 56 kV, and the influences of PLGA/PCL weight ratio on the spinning solutions and the obtained NFMs were identified.

Solution viscosity and conductivity

It is well known that the solution viscosity and conductivity have significant impacts on the yield and morphology of the electrospun NFMs.[50] The viscosities and conductivities of solutions with different PLGA/PCL weight ratios were indicated in Figure 3. It could be seen that with the decrease of PLGA contents, the solution viscosity decreased accordingly because of larger molecular weight of PLGA than that of PCL, while the conductivity first rose and then fell, which might be the result of the interaction between groups of PLGA and PCL. Furthermore, as PLGA contents enhanced, the formation of PLGA molecular chain of unconventional line groups increased and tangled sufficiently, resulting in the enhanced frictional resistance during the movement of large molecules, thus increasing the solution viscosity.[51] When PLGA/PCL weight ratio was 6:4, the spinning solution had moderate viscosity and the highest conductivity, leading to the easier preparation of PLGA/PCL NFMs.

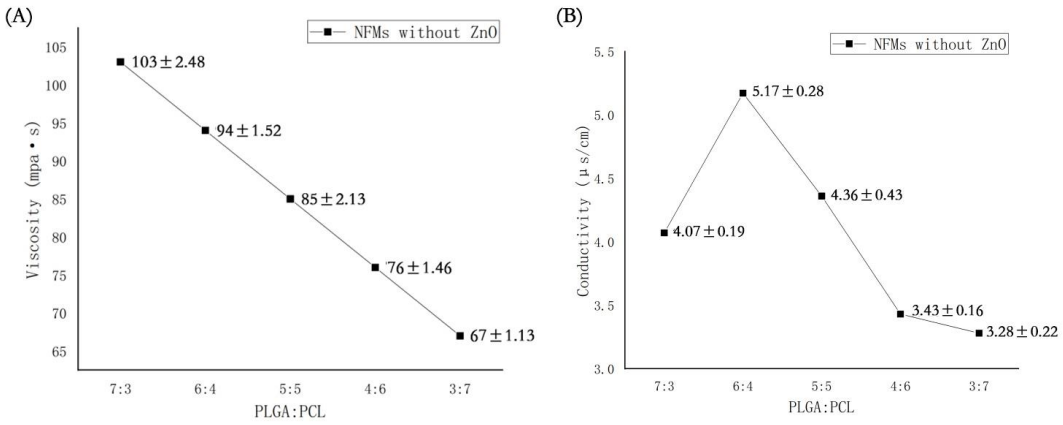

Figure 3 Viscosities (A) and conductivities (B) of spinning solutions with different PLGA/PCL weight ratios.

Yield of NFMs

The yields of NFMs with different PLAG/PCL weight ratios obtained by the OSFSE apparatus were demonstrated in Figure 4. It was found that as PLGA contents grew, the yield of NFMs first rose and then dropped, which was in accordance with the change trend of the solution conductivity. This reason was that with the increase of solution conductivity the electric field force on the solution surface enhanced, which caused more jets to be produced from the solution surface and enlarged the output of NFMs. In addition, when the solution viscosity was relatively larger, the tangle and penetration of the molecular chain were enhanced, resulting in the increase of NFMs yield. Therefore, when PLAG/PCL weight ratio was 6:4, the yield reached the maximum value (30.84±1.98 g/h).

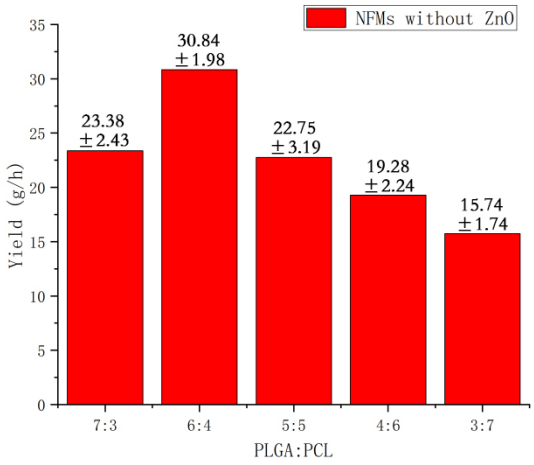

Figure 4 Yields of NFMs with different PLGA/PCL weight ratios.

Morphology of NFMs

SEM pictures and diameter distributions of NFMs with different PLAG/PCL weight ratios were indicated in Figure 5. It was obvious that when PLAG/PCL weight ratio was 5:5, there appeared some particles on the surface of NFMs. And as PLGA contents further decreased, the numbers of particles and beads appeared on the surface of NFMs increased gradually, due to the decrease of the solution viscosity. It was because continuous and smooth nanofibers couldn't be produced from solutions with low viscosity.[52] When the weight ratio was 6:4, the NFM presented the best morphology, the smallest average diameter of nanofibers, and the most uniform diameter distribution of nanofibers, due to the moderate viscosity and the highest conductivity of the spinning solution.

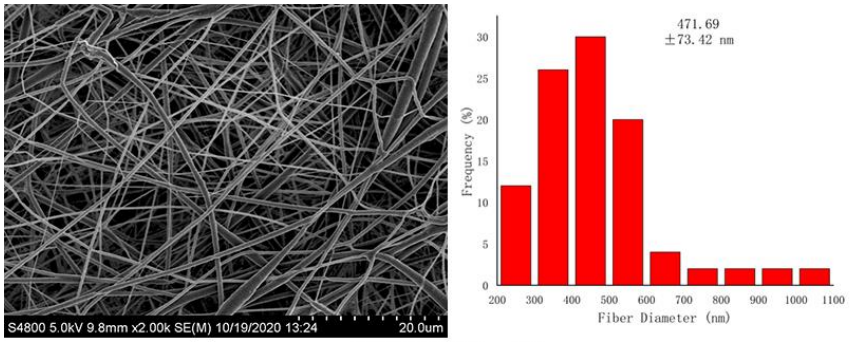

(A) PLGA:PCL = 7:3

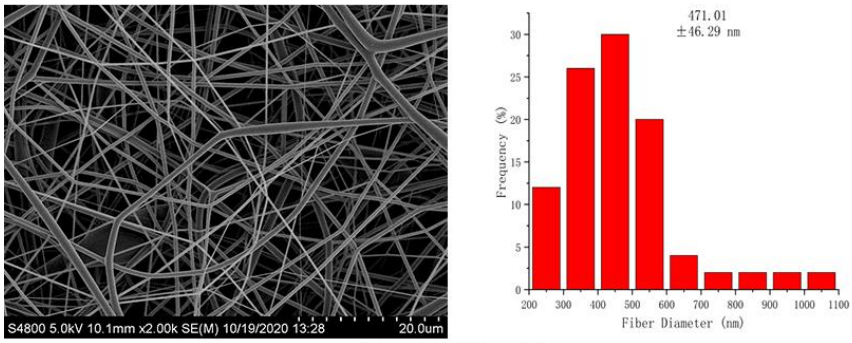

(B) PLGA:PCL = 6:4

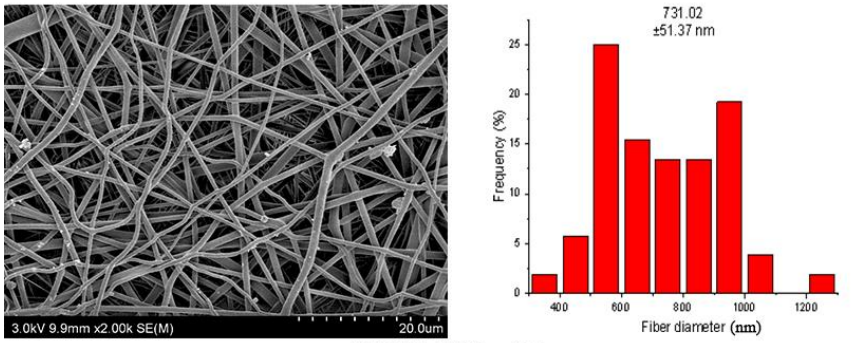

(C) PLGA:PCL = 5:5

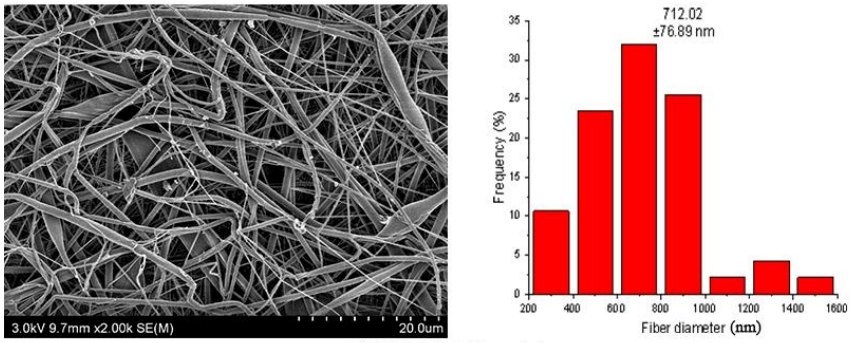

(D) PLGA:PCL = 4:6

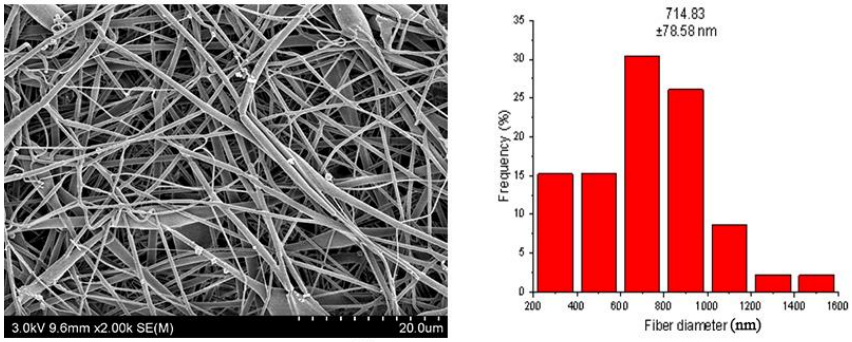

(E) PLGA:PCL = 3:7

Figure 5 SEM pictures and diameter distributions of NFMs with different PLGA/PCL weight ratios.

WCA of NFMs

WCA is often applied to exhibit the wettability of NFMs. Figure 6 revealed the WCA values of electrospun NFMs with different PLGA/PCL weight ratios. It was found that all NFMs were hydrophobic materials and their WCAs ranged from 112.98° to 121.45°. And the NFM with the weight ratio of 6:4 (PLGA: PCL) had the smallest WAC, which also meant the NFM had a relatively smooth and flat surface compared with other NFMs. It was because the rougher the surface was, the more hydrophobic the material was.

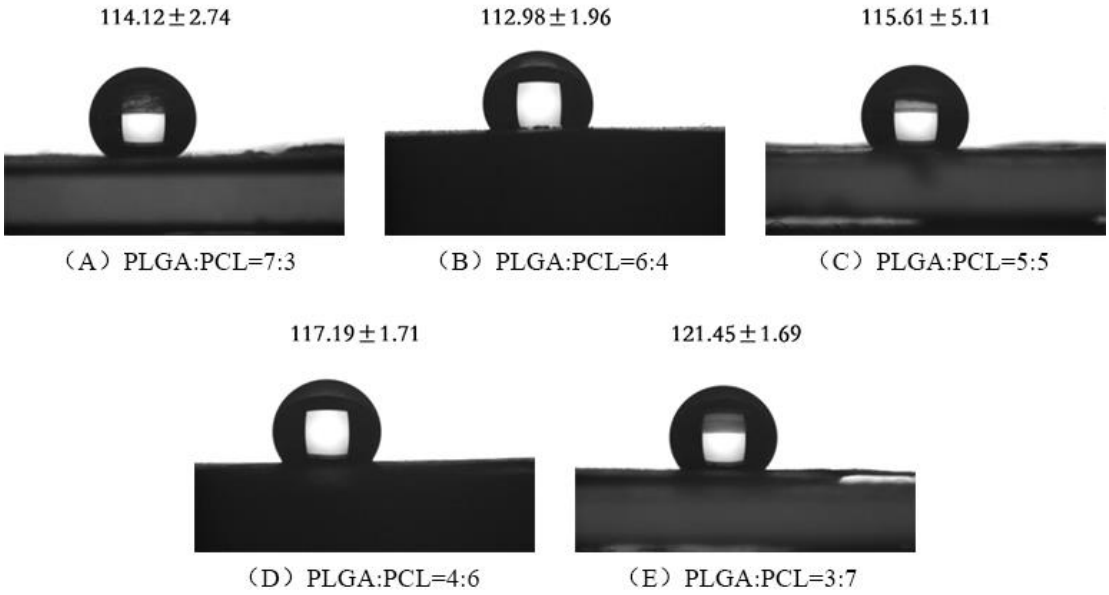

Figure 6 Images of measuring water contact angle of NFMs with different PLGA/PCL weight ratios.

Comprehensively considering the yield, morphology and properties of the prepared NFMs, the optimal PLGA/PCL weight ratio of 6:4 was determined and selected in the following study.

Effects of the additive content of ZnO

ZnO/PLGA/PCL NFMs with a weight ratio of 6:4 (PLGA: PCL) were fabricated using OSFSE apparatus at 56 kV, and the effects of ZnO contents on the spinning solutions and the prepared NFMs were studied.

Solution viscosity and conductivity

Figure 7 presented the viscosity and conductivity of the solutions with various ZnO contents. It was obvious that the addition of nano-ZnO and CA had minor influence on the solution viscosity due to their low molecular weight and dosage, and the addition of them improved the solution conductivity because of the increase of conductive particles in the solution.

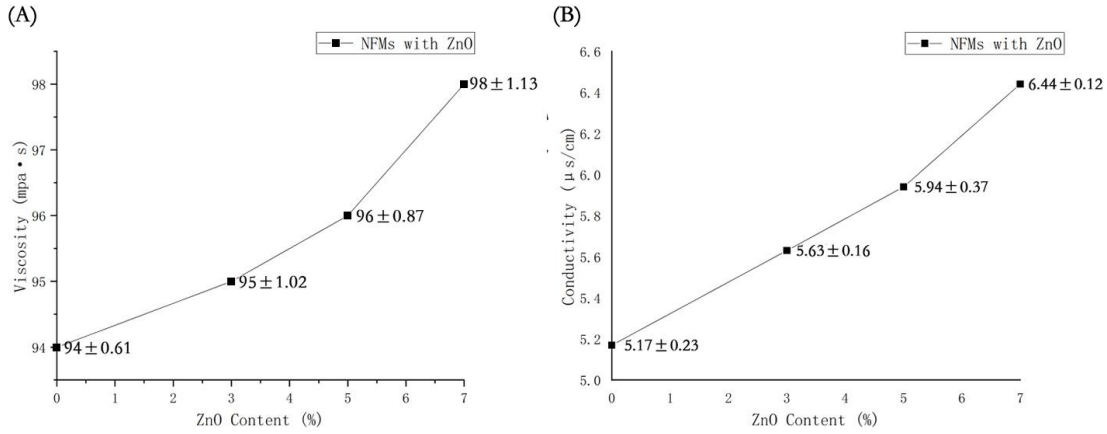

Figure 7 Viscosities (A) and conductivities (B) of spinning solutions with different ZnO contents.

Yield of NFMs

The addition of ZnO had a positive influence on increasing the yield of NFMs. As ZnO contents grew, the number of conductive particles in the spinning solution enhanced, leading to the increase of the electric field force on the solution surface and more jets generated from the solution surface. However, when ZnO contents are too high (5 wt% and 7 wt%), the surface charge density of the jets was too large, resulting in the fierce repulsion force between the charged jets, which would make the jets become unstable and expand outward. Therefore, it was difficult to collect nanofibers, leading to lower yield of NFMs, as shown in Figure 8. When ZnO content was 3 wt%, the yield of NFMs reached the maximum value of 34.25 g/h.

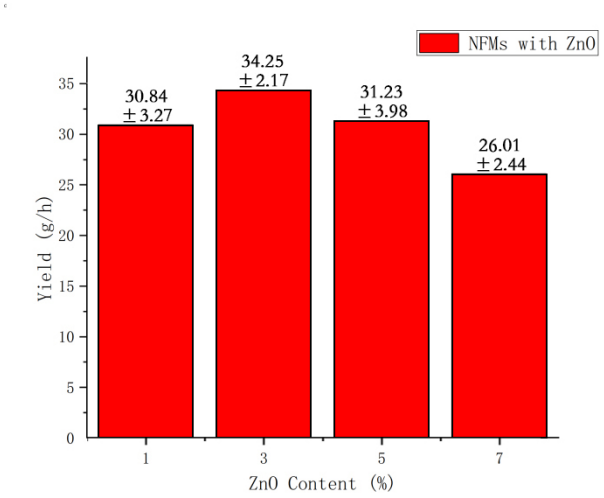

Figure 8 Yields of NFMs with different ZnO contents.

Morphology of NFMs

Figure 9 demonstrated SEM images and diameter distributions of NFMs with different ZnO

contents. It could be found the addition of ZnO would make the average diameter of nanofibers bigger due to higher solution viscosity. Moreover, with the increase of ZnO contents, the average diameter of nanofibers decreased because of the increase of solution conductivity, but the diameter distribution of nanofibers became more non-uniform. This was because the surface charge density of the jets was too high due to the high ZnO contents, which resulted in the strong repulsive force between the charged jets and made the jets become uneven and unstable. Accordingly, when ZnO content was 3 wt%, the diameter distribution of nanofibers was the most uniform.

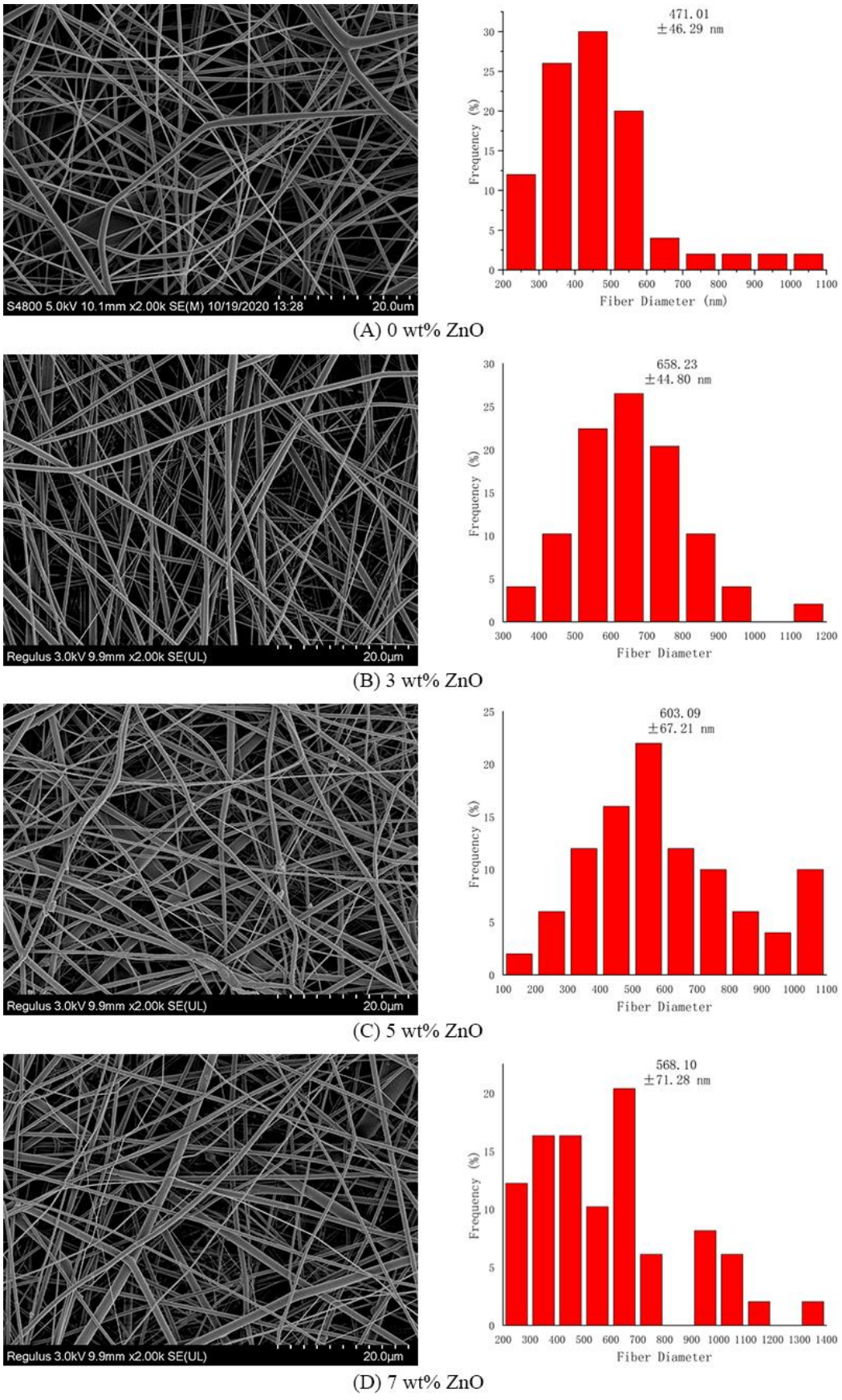

Figure 9 SEM images and diameter distributions of NFMs with different ZnO contents.

EDS analysis of NFMs

Table 1 and Figure 10 showed the content and distribution of different elementary substance of NFMs with varying concentration of ZnO. It could be seen from Table 1 that as ZnO concentration grew in the spinning solution the content of Zn element in the NFMs enhanced. As shown in Figure 10, when the concentration of ZnO was 3%, CA played a great role in inhibiting the agglomeration of nanoparticles, and ZnO nanoparticles were uniformly dispersed in NFMs. However, when the concentrations of ZnO were 5% and 7%, it was found that ZnO nanoparticles tended to agglomerate, which was likely to have a negative influence on the antibacteria effect of NFMs.

ZnO Content	**Atomic Percent of Elementary substance (%)**			
(wt%)	O	N	C	Zn
0	14.47	8.65	76.88	0
3	23.85	0.26	75.81	0.07
5	16.80	7.90	75.19	0.11
7	19.82	7.87	72.16	0.15

Table 1 Atomic Percent of elemental composition of NFMs with different ZnO contents.

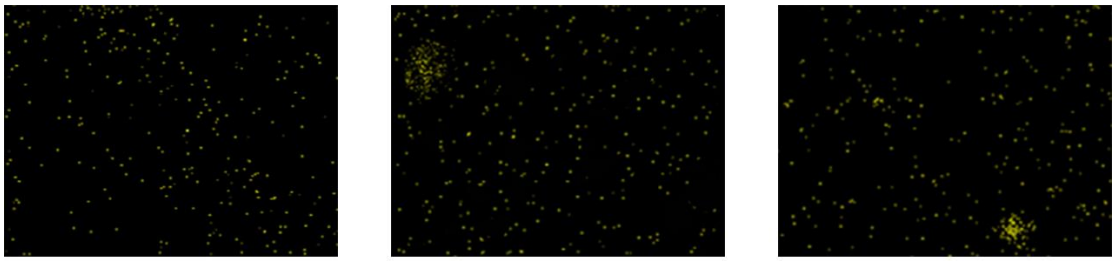

(A) 3 wt% ZnO (B) 5 wt% ZnO (C) 7 wt% ZnO

Figure 10 Zn element distribution of NFMs with different ZnO contents.

ATR-FTIR analysis of NFMs

ATR-FTIR characterizations of PLGA/PCL NFMs with ZnO contents of 0 wt%, 3 wt%, 5 wt% 7 wt% were shown in Figure 11. The characteristic absorption peaks were observed at 1756 cm^{-1} and 1722 cm^{-1}. The former was related to the free ester-based functional group of PLGA, and the latter was associated with the conjugated ester-based functional group of PCL.[53,54] The characteristic peaks appeared at 1088 cm^{-1}, at 1188 cm^{-1} and at 2948 cm^{-1} were attributed to C-O-C stretching, C=C stretching and -CH_2 asymmetric stretching, respectively, which provided further evidence for the presence of PCL.[49] These peaks could be observed in all NFMs, indicating that the addition of nano ZnO and CA could not destroy the chemical properties of PLGA/PCL. No peaks related to Zn-O stretching were found because of low concentration of ZnO. However, all the NFMs with ZnO had a wide peak at 3353 cm^{-1} (-OH stretching), which could result from water molecules absorbed by the surface of nano ZnO-CA and thereby demonstrate the existence of ZnO in NFMs.[49]

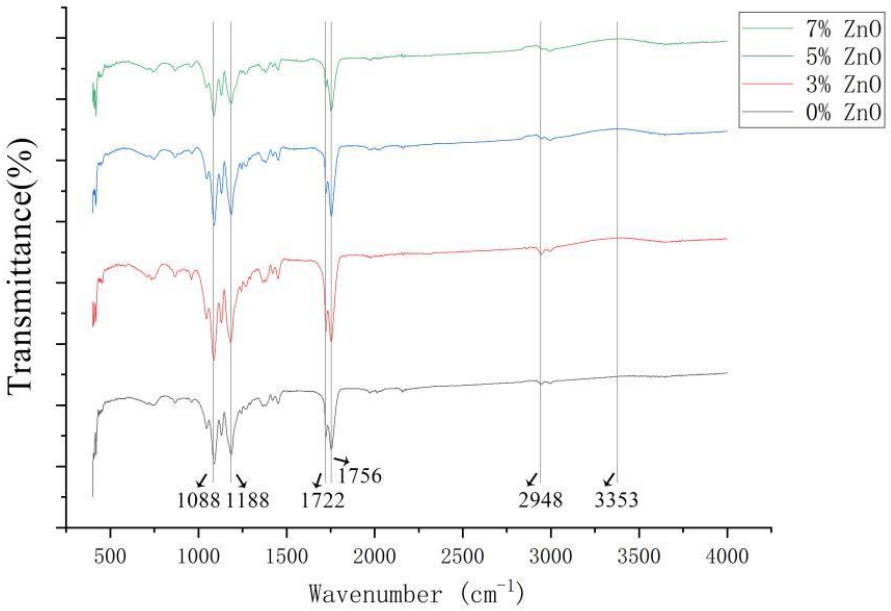

Figure 11 ATR-FTIR characterizations of NFMs with different ZnO contents.

XRD analysis of NFMs

The XRD patterns of PLGA/PCL NFMs with different ZnO contents were exhibited in Figure 12. There are characteristic diffraction peaks near 2θ= 22.1° and 23.8°, which were in accordance with α crystalline form (110) and β crystalline form (200) of PCL [49], respective. With the increase of nano ZnO and CA contents, the XRD pattern of PLGA/PCL/ZnO NFMs revealed that the crystalline phase of PCL did not change, but the characteristic peaks weakened. This was because that nano ZnO was dispersed in the PCL polymer chains after adding nano ZnO into the spinning solution and fully stirring, which damaged the structure of PCL polymer chain regulation, increased the amorphous region of PCL and reduced the crystallinity of PCL. The XRD patterns of NFMs containging ZnO all showed peaks at 31.8° (100), 34.4° (002) and 36.6° (101), illustrating the crystalline form of ZnO.

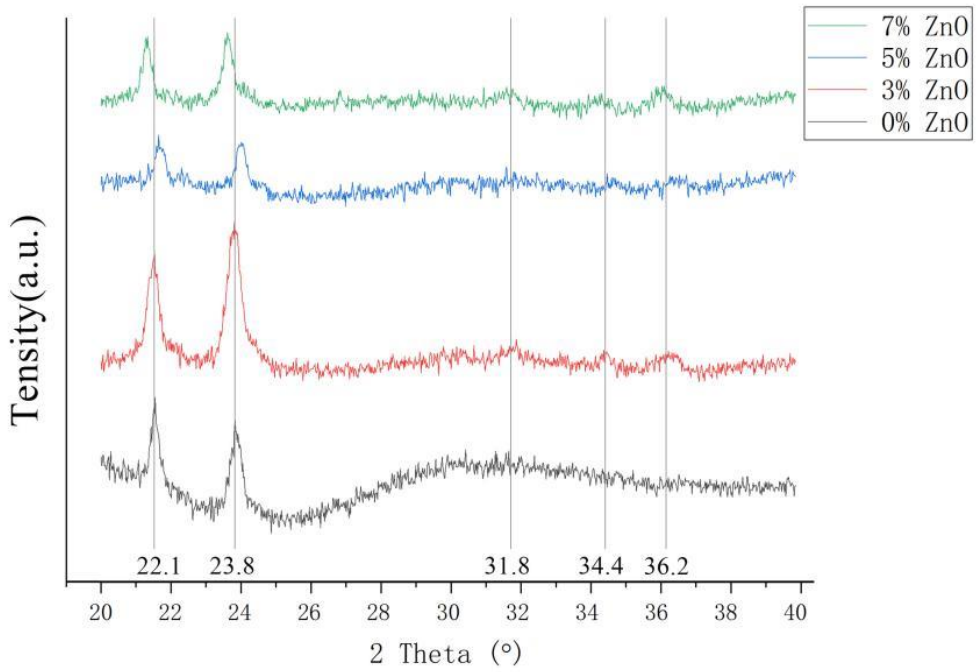

Figure 12 XRD patterns of NFMs with different ZnO contents.

Mechanical property of NFMs

ZnO Content (wt%)		0	3	5	7
Thickness	average value (um)	132.5	129.0	126.9	164.4
	stranded deviation	10.6	4.58	3.3	4.6
Breaking strength	average value (cN/cm)	67.12	110.78	106.76	88.02
	stranded deviation	5.23	3.98	1.07	3.17
Elongation at Break	average value(%/cm)	26.16	19.49	20.7	24.62
	stranded deviation	5.18	0.57	2.34	3.74

Table 2 Mechanical property of NFMs with different ZnO contents.

The mechanical properties of NFMs with the various concentration of ZnO were shown in Table.3. It was presented that the addition of ZnO would enhance the mechanical properties, however, as ZnO contents grew, the breaking strength dropped gradually and the elongation at break increased. This was because with the increase of ZnO contents, the average nanofiber diameter reduced and the diameter distribution of nanofibers became more non-uniform, as indicated in Figure 9. Therefore, the NFM with ZnO concentration of 3 wt% exhibited the best mechanical properties, due to its largest average diameter of nanofibers and the most uniform diameter distribution of nanofibers.

WAC of NFMs

Figure 11 showed the representative images of WAC during the measurement and their corresponding WAC value. After adding ZnO and CA, NFMs still remained hydrophobic and their WACs gradually decreased from 112.98° to 104.14°. This was because that nano-ZnO and CA contained hydroxyl groups,[49] which was benefit to improve the hydrophily of materials.

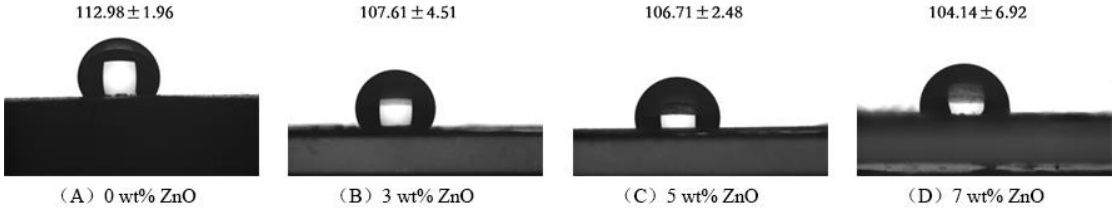

Figure 13 Images of measuring WAC of NFMs with different ZnO contents

Antibacterial activity of NFMs

Figure 12 showed the antibacterial properties of ZnO/PLGA/PCL NFMs with different ZnO contents against *E. coli* and *S. aureus*. The standard cotton cloth was used as a control. The results illustrated that the addition ZnO could greatly improve the antibacterial property of NFMs, and the NFMs containing ZnO all had excellent antibacterial activities against *E. coli* and *S. aureus*. The higher the content of ZnO was, the better the antibacterial ability of NFM was. When the concentration of ZnO was 3 wt%, the antibacterial rates against *E. coli* and *S. aureus* could still reach 95.3% and 95.7%, respectively.

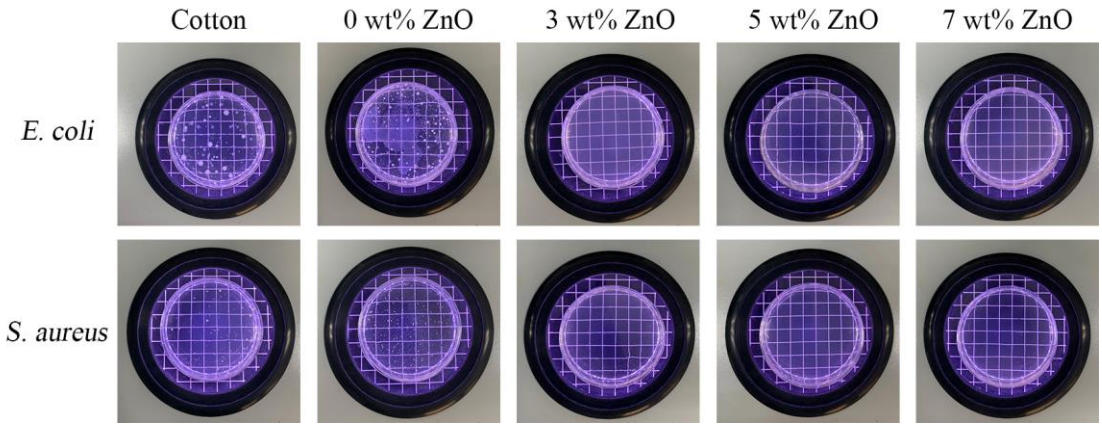

Figure 14 Images of antibacterial status of NFMs with different ZnO contents against *S. aureus* and *E. coli.*

ZnO Content		3%	5%	7%
Antibacterial Rate	*E. coli*	95.3%	96.4%	96.9%
	S. aureus	95.7%	96.2%	96.4%

Table 3 Antibacterial rates of NFMs with different ZnO contents against *S. aureus and E. coli*.

Conclusion

In this paper, an OSFES apparatus was utilized to fabricate high-quality and high-output

ZnO/PLGA/PCL NFMs for antibacterial materials. Firstly, the weight ratio of PLGA and PCL on the solution viscosity and conductivity as well as the yield, morphology and wettability of the obtained PLGA/PCL NFMs were studied, and the optimal weight ratio was determined. The results indicated that when the weight ratio of PLGA and PCL was 6:4, the quality of the prepared NFM was best, and its yield reached the maximum value of 30.84 g/h.

Afterwards, the effects of ZnO contents on the spinning solution properties as well as the yield, morphology, wettability, mechanical property and antibacterial performance of ZnO/PLGA/PCL NFMs with the optimal PLGA/PCL weight ratio of 6:4 was discussed. The results illustrated that the addition of ZnO could improve the yield, mechanical property and antibacterial performance of NFMs, and with the increase of ZnO contents the antibacterial ability of NFM enhanced. In addition, the ZnO/PLGA/PCL NFM with 3 wt% ZnO had the highest yield, the most uniform diameter distribution and Zn element distribution, the smallest WCA, as well as better mechanical and antibacterial performances. Comprehensively considering the yield, morphology and properties of the prepared ZnO/PLGA/PCL NFMs, 3% ZnO will be selected as the optimal parameter in future study.

Acknowledgement

The work is supported financially by National Natural Science Foundation of China (Grant No. 11672198), Jiangsu Higher Education Institutions of China (Grant No. 20KJA130001), Six Talent Peaks Project of Jiangsu Province (Grant No. GDZB-050), and PAPD (A Project Funded by the Priority Academic Program Development of Jiangsu Higher Education Institutions).

References

[1] Sofokleous P. ; Stride E.; Edirisinghe M. *Pharm. Res.* **2013**, *30*, 1926-1938. doi:10.1016/j.ijpharm.2011.05.049

[2] Fredenberg S.; Wahlgren M.; Reslow M.; Axelsson A. *Int. J. Pharm.* **2011**, *415*, 34-52. doi:10.1016/j.ijpharm.2011.05.049

[3] Whang K.; Tsai D.C.; Nam E.K.; Aitken M.; Sprague S.M.; Patel P.K.; Healy K.E. *J. Biomed. Mater. Res.* **1998**, *42*, 491. doi: 10.1002/(sici)1097-4636(19981215)42:4<491::Aid-jbm3>3.0.Co;2-f

[4] Pan H.; Jiang H.L.; Chen W.L. *Biomaterials*. **2006**, *27*, 3209-3220. doi:10.1016/j.biomaterials.2006.01.032

[5] Shin H.J.; Lee C.H.; Cho I.H.; Kim Y.J.; Lee Y.J.; Kim I.A.; Park K.D.; Yui N.; Shin J.W. *J. Biomater. Sci. Polym. Ed.* **2006**, *17*, 103-119. doi:10.1163/156856206774879126

[6] Vasita R.; Shanmugam K.; Katti D.S. *Polym. Degrad. Stab.* **2010**, *95*, 1605-1613. doi:10.1016/j.polymdegradstab.2010.05.032

[7] Liu H.; Wang S.; Qi N. *J. Appl. Polym. Sci.* **2012**, *125*, E468-E476. doi:10.1002/app.36757

[8] Bei J.Z.; Wang W.H.; Wang Z.F.; Wang S.G. *Polym. Adv. Technol.* **1996**, *7*, 104-107. doi:10.1002/(sici)1099-1581(199602)7:2<104::Aid-pat443>3.0.Co;2-0

[9] Tay B.Y.; Zhang S.X.; Myint M.H.; Ng F.L.; Chandrasekaran M.; Tan L.K.A. *J. Mater. Process. Technol.* **2007**, *182*, 117-121. doi:10.1016/j.jmatprotec.2006.07.016

[10] Rouxhet L.; Duhoux F.; Borecky O.; Legras R.; Schneider Y.J. *J. Biomater. Sci. Polym. Ed.* **1998**, *9*, 1279-1304. doi:10.1163/156856298x00398

[11] Biresaw G.; Carriere C.J. *J. Appl. Polym. Sci.* **2002**, *83*, 3145-3151. doi:10.1002/app.10178
[12] Zhang M.; Xu W.-Y.; Wang J.-M.; Luan J.-S.; Dong H.-N.; Zhang Y.-J.; Li X.-Q.; Sun D.-H. *J. Appl. Polym. Sci.* **2015**, *132*, 23. doi:10.1002/app.42030
[13] Ma L.; Shi X.; Zhang X.; Dong S.; Li L. *PHYS. STATUS. SOLIDI. A.* **2019**, *216*, 1900307. doi:10.1002/pssa.201900379
[14] Liu S.-J.; Kau Y.-C.; Chou C.-Y.; Chen J.-K.; Wu R.-C.; Yeh W.-L. *J. Membr. Sci.* **2010**, *355*, 53-59. doi:10.1016/j.memsci.2010.03.012
[15] Makadia H.K.; Siegel S.J. *Polymers*. **2011**, *3*, 1377-1397. doi:10.3390/polym3031377
[16] Miao R.D.; Yu H.; Wu D.F.; Zhang M.; Li X. *CN. Plastic Ind*. **2009**, *37*, 50-53. doi:10.3321/j.issn:1005-5770.2009.09.013
[17] Jian C.; Gong C.; Wang S.; Wang S.; Xie X.; Wei Y.; Yuan J. *Eur. Polym. J.* **2014**, *55*, 235-244. doi:10.1016/j.eurpolymj.2014.04.003
[18] Chen H.G.; Bei J.Z.; Wang S.G. *Acta Polym. Sin.* **2000**, *5*, 626-631.
[19] Hu S.-d.; Wang C.; Cai M.-t.; Zhai S.-y.; Luo X.-l. *Acta Polym. Sin.* **2014**, *6*, 782-788. doi:10.3724/sp.J.1105.2014.13364
[20] Li Y.F.; Wang B.H.; Huang W.X.; Tu M.S.; Wang X.D.; Wang D. *New Chem. Mater*. **2002**, *6*, 44-46. doi:10.3969/j.issn.1006-3536.2002.06.011
[21] Kuang H.J.; Yang L.; Xu H.Y.; Zhang W.Y. *Chin. J. Pharmacol. Toxicol*. **2015**, *29*, 153-157. doi:10.3867/j.issn.1000-3002.2015.01.024
[22] Brayner R.; Ferrari-Iliou R.; Brivois N.; Djediat S.; Benedetti M.F.; Fievet F. *Nano Lett.* **2006**, *6*, 866-870. doi:866-870. 10.1021/nl052326h
[23] Zhang Z.J.; Wang Z.H.; Sun L.; Zhao Y.B. *Chem. Res*. **2016**, *27*, 12-20. doi:10.14002/j.hxya.2016.01.002
[24] Mallakpour S.; Abdolmaleki A.; Rostami M. *Polym. Plast. Technol. Eng*. **2014**, *53*, 1615-1624. doi:10.1080/03602559.2014.919644
[25] Hell S.; Ohkawa K.; Amer H.; Potthast A.; Rosenau T. *Nanomaterials*. **2020**, *10*, 671. doi:10.3390/nano10040671
[26] Kang Y.-M.; Kim K.-H.; Seol Y.-J.; Rhee S.-H. *Acta Biomater*. **2009**, *5*, 462-469. doi:10.1016/j.actbio.2008.07.004
[27] P. Lu, Y.-L. Hsieh, *ACS Appl. Mater. Interfaces*. **2010**, *2*, 2413-2420. doi:10.1021/am1004128
[28] Li C.; Li Q.; Ni X.; Liu G.; Cheng W.; Han G. *Materials*. **2017**, *10*, 572. doi:10.3390/ma10060572
[29] Sequeira R.S.; Miguel S.P.; Cabral C.S.D.; Moreira A.F.; Ferreira P.; Correia I.J. *Int. J. Pharm.* **2019**, *570*, 118640. doi:10.1016/j.ijpharm.2019.118640
[30] Sill T.J.; von Recum H.A. *Biomaterials*. **2008**, *29*, 1989-2006. doi:10.1016/j.biomaterials.2008.01.011
[31] Yang F.; Murugan R.; Wang S.; Ramakrishna S. *Biomater*. **2005**, *26*, 2603-2610. doi: 10.1016/j.biomaterials.2004.06.051
[32] Teixeira M.A.; Paiva M.C.; Amorim M.T.P.; Felgueiras H.P. *Nanomater*. **2020**, *10*, 557. doi:10.3390/nano10030557
[33] Liu Y.; Liang X.; Zhang R.; Lan W.; Qin W. *Polymers*. **2017**, *9*, 464. doi:10.3390/polym9100464
[34] Detta N.; Puppi D.; Chiellini F.; Chiellini E. *Tissue Eng. Part A*. **2008**, *14*, 898-898. doi:10.1016/j.biopha.2008.07.008

[35] Varabhas J.S.; Chase G.G.; Reneker D.H. *Polymer*. **2008**, *49*, 4226-4229. doi:10.1016/j.polymer.2008.07.043
[36] Jiang R.; Yan T.; Wang Y.-Q.; Pan Z.-J. *J. Appl. Polym. Sci.* **2020**, *137*, 49053. doi:10.1002/app.49053
[37] Li J.J.; Ji J.; Wang L.Q. *Adv. Text. Technol*. **2019**, *27*, 91-96. doi:10.19398/j.att.201803008
[38] Jahan I.; Wang L.; Wang X. *Macromol. Mater. Eng*. **2019**, *304*, 1800588. doi:10.1002/mame.201800588
[39] Huang C.; Niu H.; Wu J.; Ke Q.; Mo X.; Lin T. *J. Nanomater*. **2012**, *2012*. doi:10.1155/2012/473872
[40] Moreira J.B.; Lim L.-T.; Zavareze E.d.R.; Guerra Dias A.R.; Vieira Costa J.A.; de Morais M.G. *Food Hydrocoll*. **2019**, *93*, 131-136. doi:10.1016/j.foodhyd.2019.02.015
[41] Ahmed A.; Xu L.; Yin J.; Wang M.; Khan F.; Ali M. *Fibers Polym*. **2020**, *21*, 1945-1955. doi:10.1007/s12221-020-1109-9
[42] Yin J.; Xu L. *Int. J. Biol. Macromol*. **2020**, *160*, 352-363. doi:10.1016/j.ijbiomac.2020.05.211
[43] Fang Y.; Xu L. *Beilstein J. Nanotechnol*. **2019**, *10*, 2261-2274. doi:10.3762/bjnano.10.218
[44] Fang Y.; Xu L.; Wang M.D. *Nanomaterials*. **2018**, *7*, 8. doi:10.3390/nano8070471
[45] Shao Z.B.; Yu L.; Xu L.; Wang M. *Nanoscale Res. Lett.* **2017**, *12*, 1-9. doi:10.1186/s11671-017-2240-4
[46] Yu L.; Shao Z.B.; Xu L.; Wang M.D. *Polymers*. **2017**, *9*, 658. doi:10.3390/polym9120658
[47] Gao J.C.; Chen S.Y.; Tang D.; Jiang L.; Shi, J.; Wang S.F. *Trans. Tianjin Univ*. **2019**, *25*, 152-160. doi:10.1007/s12209-018-0152-8
[48] Thi N.; Lee H.; Byong-Taek *J. Mater. Sci. Mater. Med*. **2010**, *21*, 1969-1978. doi:10.1007/s10856-010-4048-y
[49] Ding W. Study on the preparation, properties and spinnability of Poly(ε-Caprolactone)/ZnO-CA based on antibacterial nanocomposites, Donghua Univ, **2018**.
[50] Li N.; Qin X.H.; Lin L. *Polym.Eng.Sci.* **2008**, *48*, 2362-2366. doi:10.1002/pen.21188
[51] Zou S.; Zhao J.S.; Chen C. *Henan Technonol*. **2019**, *5*, 75-77. doi:10.3969/j.issn.1003-5168.2019.05.030
[52] Saikat Sinha Ray, Shiao-Shing Chen, Nguyen Cong Nguyen, Hau Thi Nguyen, *Micro Nano Technol.* **2019**, *9*, 247. doi:10.1016/ B978-0-12-813926-4.00014-8
[53] Gaharwar A.K.; Schexnailder P.J.; Jin Q.; Wu C.J.; Schmidt G. *ACS Appl. Mater. Interfaces.* **2010,** *2*, 3119-3127. Doi:10.1021/am100609t
[54] Bottino M.C.; Thomas V.; Janowski G.M. *Acta Biomater.* **2011**, *7*, 216-224. doi:10.1016/j.actbio.2010.08.019